A FITTING TOOL FOR RELATIVISTIC DISTORTIONS IN KERR BH SPECTRA

A. MARTOCCHIA
SISSA-ISAS, Via Beirut 2/4, I–34014 Trieste, Italy; E-mail: martok@sissa.it

G. MATT
Dipartimento di Fisica, Università degli Studi "Roma Tre", Via della Vasca Navale 84, I–00146 Roma, Italy; E-mail: matt@haendel.fis.uniroma3.it

V. KARAS
Astronomical Institute, Charles University Prague, V Holešovičkách 2, CZ–180 00 Praha, Czech Republic; E-mail: vladimir.karas@mff.cuni.cz

Recently, much attention has been devoted to the relativistic distortions of Kα iron line profiles from Active Galactic Nuclei and Galactic Black Hole Candidates. However, computations have been usually performed without regard to the effects on other important features, e.g. the underlying reflected continuum, and fits to real data have been usually performed adopting ad hoc assumptions on the sources geometry and emissivity. We developed an XSPEC model to allow fits of data of any spectral feature under many possible different geometrical and physical hypotheses. Some practical examples of the code usage are made with regard to well-known Kerr BH candidate sources.

1 Introduction

Complex emission features in the X-ray spectra of Active Galactic Nuclei (AGN) and galactic Black Hole Candidates (GBHCs), with shapes and energies most naturally explained in terms of relativistic effects, have recently been discovered by satellites. Such relativistic distortions in the X-ray spectra of candidate BH systems are a fundamental diagnostic to probe the effects of strong gravity. Fully-relativistic calculations may even help to distinguish static from rotating BHs (e.g. Martocchia 2000, and references therein).

The interest in such high-energy spectral distortions arised especially after the detection of the broad, asymmetric profile of the iron Kα fluorescent line in the X-ray data of the Seyfert galaxy MCG–6-30-15 (Tanaka *et al.*, 1995), whose shape is thought to be due to general-relativistic effects taking place at just a few gravitational radii from the event horizon of a central supermassive BH. Also the large equivalent width of the fluorescent Kα line and the position of its centroid energy may be understood if the line is produced in a medium with fast rotational motion, very near to a BH (Fabian *et al.*, 1989; Laor 1991; Martocchia & Matt 1996; Martocchia, Karas & Matt 2000; and references therein).

Currently, both the continuum and the iron Kα line emission from accretion discs around rotating black holes are being investigated under simplifying assumptions on the geometry of the sources and the physical processes which produce the X-ray features. A self-consistent treatment of the problem must take into account the general-relativistic effects acting also on the primary, illuminating flux, as well as the complex physical conditions (density, ionization, etc.) under which the X-ray reprocessing takes place in the accretion disc. While the latter issue is very complex and still subject to preliminary studies (e.g. Done & Nayakshin, 2000), the GR anisotropy of the illuminating flux can be now treated in a satisfactory way, even if still on the base of simplified toy-models of the geometry of the primary flux emitting region (e.g. Martocchia & Matt 1996).

Synthetic spectra of the radiation which is reflected from the BH accretion disc – iron fluorescent line and Compton-reflected continuum hump – have to be compared with the data obtained by X-ray telescopes. We have developed a fitting tool, named kerrspec, which works within the XSPEC package for fitting data. The three sources we are dealing with for this presentation are two Sy-1 galaxies (MCG–6-30-15 and NGC 3516) and a galactic *microquasar* (GRS 1915+105). The two Seyferts have been chosen because their *ASCA* spectra show the best-resolved broad iron lines. There are more objects of the same kind where such features have been detected, but for the moment none of them can be very useful to test relativistic distortions. In the present contribution, after describing the fitting technique that we have recently developed, we illustrate the new results we obtained for the selected sources.

2 Technical details

Fully-relativistic integration of photon paths in the spinning BH (Kerr) metric is needed to compute spectral distortions from accreting BH systems. In such studies, the reflector is usually considered as a perfectly thin, cold disc extending on the equatorial plane from the innermost stable orbit r_{ms} to some outer radius, and the disc emissivity law is either computed on the base of a rigorous treatment of the primary illumination, or parametrized as a simple power-law function of the distance. Here we adopted the first of the two methods, fully taking into account the GR effects on the trajectories of the primary photons – which are emitted from a central pointlike source located at a distance h on the BH rotation axis ("lamp-post" model; e.g. Martocchia & Matt 1996) – and their reprocessing in the disc matter, which re-emits them via Compton-reflection and fluorescence – modelled through a Montecarlo code (Matt *et al.*, 1991).

The computations of "synthetic" line profiles and spectra can subsequently be employed to fit observational data. To this aim, a large number of spectra has to be computed in a short time, even if one restricts the parameter region as far as possible. Thus a large number of geodesics has been pre-calculated (Karas *et al.* 1992) and stored in a catalogue, where they can be accessed fastly. We gave particular importance to the photon trajectories very near to the BH horizon (below $6m$), because the computed line profiles are strongly sensitive to the radius of the innermost emitting orbit, especially if the emissivity varies rapidly with the radius (case of small h; cp. Martocchia, Karas & Matt 2000). The innermost emitting orbit is usually identified with the marginally stable one, which depends on the BH angular momentum.

We used our newly-developed tool kerrspec in the XSPEC package for X-ray data analysis.[a] In our tool, the radial dependence, the angular dependence as well as the frequency dependence (local spectrum) of the local emission can be given as inputs; after fixing the desired resolution in the image plane, the geodesics corresponding to all image points are sorted-out from the catalogue.

The kerrspec routine allows to adjust or fit over many different parameters and assumptions. The **spacetime** can be that of a static or of a spinning BH. A sub-section of the catalogue can be constructed for every a (BH normalized spin parameter) of interest. Obviously, the **inclination of the distant observer** (i) may also be varied. In these preliminary computations we used 10 catalogues, for $\mu = \cos(i)$ varying with regular steps $\delta\mu = 0.1$. As far as the **disc model** is concerned, for the initial purposes we have restricted ourselves to the case of geometrically thin discs; however, because in the catalogues the whole shape of each geodesic is stored, it is easy to consider a different disc geometry, i.e. some law for the disc thickness, in the form of a function $z(r)$ ($z = 0$ for an equatorial disc). Also, a radial component for the velocity of the accreting matter, for instance an advection velocity component, can be easily introduced into the model. Of course, the **disc size** (inner edge r_1, outer edge r_2) plays an important role in determining the final line shape, especially due to the radius of the inner edge. The **local radiation flux** $F(r)$ may follow a power-law dependence ($F_q(r) \propto r^{-q}$, $q = const$), a standard Page & Thorne model (1974; see also Novikov & Thorne, 1973), or the emissivity law which results from a disc illumination from a central source (Martocchia & Matt 1996). In the latter case – which has been used here – the parameter is h; the corresponding emissivity law is stored in a file. The **local spectrum** can be a Gaussian or a Dirac's delta function in the case of the fluorescent features. In the computations we are illustrating here, a Delta function has been used; however, the code also allows to compute distortions on numerically computed profiles, and on broader spectra – on the base of the Montecarlo computations by Matt *et al.* (1991) – in order to self-consistently take into account the underlying reflected continuum, or any other analytical/numerical form for the local spectrum. Finally, the **angular dependence of the local emissivity**, including possibly a limb-darkening law, can be varied, too. We examined the functional forms for fluorescent and Compton-reflected emission given by Ghisellini *et al.* (1994) and the numerically-derived dependence from the Montecarlo computations by Matt *et al.* (1991). The latter is adopted for the fits presented in the following.

Thus, the fitting parameters of kerrspec have obvious meaning, apart from those which determine the resolution in the image plane, and therefore the quality of the calculated spectrum together with the required computing time. The gravitational redshift, as well as other parameters necessary to set the numerical precision and computational time, are contained in the code itself and auxiliary files.

3 Fitting real data

The usage of the kerrspec model in the XSPEC environment is analogous to the other models of spectral components included in this software. At the beginning

[a] http://heasarc.gsfc.nasa.gov/docs/xanadu/xspec/manual/manual.html

of a fit, the routine asks for the local spectrum to be used, and then starts fitting data. Typically, the code takes a few hours to fit a spectrum employing curved geodesics in the very vicinity of the BH, i.e. accounting for radiation emitted at distances of the order of m from the event horizon.

In this section we present the first results obtained fitting X-ray data with kerrspec. We considered some of the best-known galactic and extragalactic BH candidate sources, paying attention to relativistic distortions on the iron line profiles. The computations we describe in this chapter had two main scopes: first, to test the newly developed numerical tool; secondly, to see whether the fast-spinning BH assumption is required by the data or not. More preliminary fits have been performed including the underlying reflection continuum; however, these fits should be repeated more carefully and with a complete coverage of the parameters space, due to the longer computational time required when using numerical tables for the local broad-band spectra. For all sources we assumed an optically thick, neutral, and geometrically thin Keplerian accretion disc with solar elemental abundances. The data are taken from the *ASCA* and *BeppoSAX* archives.

Let us first of all stress some more technical points which have to be considered in all fits:

- In fitting the data from the *ASCA* satellite we used only spectra from the Solid-state Imaging Spectrometer (SIS) instrument. This because of the lower energy resolution of the Gas Imaging Spectrometer (GIS; Inoue 1993). The normalization constant has been fixed to 1 for one of the two SIS instruments, and kept free for the other. All the data from this satellite have been taken from the public archive, which has been provided in a very user-friendly form by Jane Turner and Kirpal Nandra.[b]
- In the case of *BeppoSAX*, data from the LECS, MECS and PDS instruments (the latter with a fixed normalization factor 0.84 with respect to MECS data) have been used, in the intervals $0.1 \div 4.$, $1.7 \div 10.$ and $15. \div 200.$ keV, respectively. However, MECS data alone are necessary to fit in the narrow energy range where the iron line is detected.
- The iron lines have been usually fitted in the narrow interval $3.5 \div 10$ keV, after a preliminary fit on a larger energy range was made in order to constrain the properties of the continuum (powerlaw index Γ and cutoff energy E_{cut}: powerlaw) using gaussian or diskline models to account for the line. In this way the computational time for the relativistic line fits has been restricted as far as possible.
- The disc emissivity is related here to the location of the central source (parameter h). Because the emission tends to be concentrated in the central parts of the disc (corresponding to low h values), the inner emitting radius is better constrained by the fit than the outer radius.

3.1 MCG–6-30-15

This source is a bright Sy-1 galaxy where a broad and asymmetric iron line has been unambiguously detected for the first time by *ASCA* (Tanaka *et al.*, 1995). The line width corresponds to a disc matter velocity of $\sim 10^5$ km s^{-1}. It also shows

[b]The *Tartarus* database can be accessed on-line at http://tartarus.gsfc.nasa.gov.

Table 1. A summary of the results obtained with kerrspec for MCG–6-30-15 using the *ASCA* data of the July 1994 observation. The model used here is: model = wabs(powerlaw + kerrspec), the primary source height $h/m = 20$. See the text for more details.

r_1/m	r_2/m	χ^2	dof	$\chi^2_{\rm red}$
1.23 frozen	$104.6^{+60.3}_{-27.2}$	590.4	571	1.034
6 frozen	$99.9^{+59.0}_{-45.5}$	589.3	571	1.025
$7.2^{+27.0}_{-5.9}$	$204.9^{+62.2}_{-105.5}$	589.3	570	1.034

a large variability on a variety of timescales. The 2–10 keV flux varied by about 40% between the five *ASCA* pointings (e.g. Weaver *et al.*, 2000). During these observations the broad line profile varied, too. In a phase of deep minimum of the total flux the line shape was best fitted by a Kerr profile (Laor 1991) with the inner emitting radius $r_{\rm min}$ equal to the last stable orbit for a maximally rotating black hole (Iwasawa *et al.*, 1996). The equivalent width was particularly large, $\sim$1 keV. This value is about a factor three larger than that obtained with the time–averaged data which, when fitted with a Kerr profile using the model by Laor (1991), gives a best fit value for $r_{\rm min}$ of about $9m$ (Tanaka *et al.*, 1995).

Here we present our own fits to *ASCA* data of MCG–6-30-15. First, we have considered the *ASCA* observation which started on July 23rd, 1994, and lasted for 362895 s, i.e. the same used by Tanaka *et al.* (1995).[c] Assuming $a = 0.9981m$ and $cos(i) = 0.87$, we tried fitting for three different values of the inner disc radius r_1, keeping the pre-calculated best-fit continuum parameters fixed (absorber's – wabs – column density $n_H = 2.04 \times 10^{22}$ cm^{-2}, powerlaw index $\Gamma = 1.96$). The best fit is obtained for an intermediate primary source height ($h = 20m$). In this case, we get the values which are shown in table 1, and $\chi^2_{\rm red} \sim 1.03$ – while, for instance, the best fit for $h = 6m$ gives $\chi^2_{\rm red} \simeq 1.6$. We also tried including the reflection component in the local spectrum, but the χ^2 was substantially worse ($\chi^2 \gtrsim 2.3$) due to the bad constrain to the continuum parameters in this case; a better modelling will require further long-lasting computations, to be performed in the future.

We thus find that the Schwarzschild assumption is slightly favoured (see table), even if the difference with the Kerr assumption is really tiny. With our best-fit model, the line EW results to be $\sim$ 210 eV.

We also tried to fit the spectrum of the source corresponding to the 1994 deep minimum, as already analyzed by Iwasawa *et al.* (1996). The selected data were kindly provided by Kazushi Iwasawa. The resulting values of χ^2 indicate that, this time, a Kerr model is favoured with respect to a Schwarzschild (or: Schwarzschild-equivalent, i.e. just fixing $r_1 = 6m$) one, either through fixing $r_1 \equiv r_{\rm ms}$ or keeping r_1 free (then the best-fit value for r_1 is 2.44; in both cases $\chi^2_{\rm red} \simeq 1.04$). This time, the primary source had to be "lowered" ($h/m = 10$) in order to improve the fit: apparently, in this state the illuminating field is more concentrated in the inner region. We also tried introducing the Compton-reflected continuum in the local spectrum, still getting a good fit ($\chi^2_{\rm red} \simeq 1.11$), but this result needs to be checked more carefully because the parameter space (e.g. h) was not completely covered.

[c] http://tartarus.gsfc.nasa.gov/html/72013000/72013000.html

Table 2. Results of the fits performed on *BeppoSAX* data for the source MCG–6-30-15. The model used here is wabs $\times$ zedge(powerlaw + kerrspec), where the local line emission is given by a Dirac's delta function (**column I**). The best-fit results by Guainazzi *et al.* (1999) are shown in **column II**, even if a comparison should take into account that the underlying reflected component has not been included in our case. An upper ^{f} means that the parameter has been frozen.

Component	Parameter	I	II
wabs	n_H [10^{22}]	0.740 ± 0.258	0.068 ± 0.003
zedge	E_{edge} [keV]	7.6^f	7.6^f
zedge	τ_{max}	0.138 ± 0.027	$0.14^{+0.03}_{-0.05}$
zedge	z	0.008^f	0.008^f
powerlaw	Γ	2.06^f	2.06^f
powerlaw	norm [10^{-2}]	2.257 ± 0.038	–
kerrspec	a/m	0.9981^f	0.0000^f
kerrspec	$cos(i)$	0.87^f	0.87^f
kerrspec	h/m	$20.^f$	$(\epsilon \propto r^{-2})$
kerrspec	r_1/m	$7.9^{+13.3}_{-6.7}$	$7.2^{+2.6}_{-1.1}$
kerrspec	r_2/m	$100.7^{+30.3}_{-16.1}$	$1000.^f$
kerrspec	dr	$1.^f$	–
kerrspec	$dpsi$	$1.^f$	–
kerrspec	norm [10^{-3}]	1.683 ± 0.607	–
	$\mathrm{EW}_{\mathrm{K}\alpha}$ [eV]	176.	200.
	χ^2_{red}	$\frac{51.3}{40} \simeq 1.28$	$\frac{138.0}{124} \simeq 1.11$

We finally fitted the model to *BeppoSAX* data.

Guainazzi *et al.* (1999) analyzed the *BeppoSAX* data and found a broad asymmetric profile, fully consistent with the *ASCA* one, in a four-days observation which took place in the summer 1996. From the *BeppoSAX* data, the Schwarzschild BH is preferred to the Kerr's one, and $i \sim 30$ degrees. The line EW this time was ~ 200 eV; the amount of reflected continuum could be more carefully evaluated thanks to the satellite's unprecedented broad bandwidth.

Like in Guainazzi *et al.* (1999), more components were added in order to improve the best-fit χ^2 value: narrow emission lines at 0.62 and 0.86 keV, and some absorption edges (one of them at 7.6 keV). We found $n_H = 0.74 \times 10^{22}$ cm^{-2}, and a photon index $\Gamma = 2.06$.

When fitting only in the narrow interval where the iron emission is present (from 3.5 to 10. keV) the XSPEC model reduces to model = wabs $\times$ zedge(powerlaw + kerrspec). While a relatively large innermost orbit radius ($r_1 \sim 8m$) seems to be preferred again in the fit, the resulting χ^2 ($\chi^2_{\mathrm{red}} = 1.28$) is slightly larger than the Guainazzi *et al.*'s value (table 2), because the Compton-reflected component has not been included in the local spectrum.

In the next future it will be possible to use *XMM-Newton* data of MCG–6-30-15, where a broad iron line is clearly visible (Molendi *et al.* 2000).

3.2 NGC 3516

Nandra *et al.* (1999) presented an analysis of the broad Kα line in the Seyfert 1 galaxy NGC 3516, on the base of a five-day observation with the *ASCA* satellite which started on April 12, 1998. These data, which have an unprecedented signalto-noise ratio, clearly show a broad redshifted profile which resembles the well-known one in MCG–6-30-15. The best fit assuming Schwarzschild metric (Fabian *et al.*, 1989) was obtained with an inner radius $r = r_{ms} = 6m$, an inclination $i = 35^o$ (lower in the Kerr assumption) and an extremely steep emissivity, with index $q = 8$, which indicates that the line emission is very much concentrated in the innermost region; when adopting a Kerr metric (diskline model, Laor 1991) the fit is still good but not as in the Schwarzschild case; therefore the fits did not allow to really constrain the BH spin. The fit is better when an absorption feature in the red tail is included, which could be due to infalling material, being accreted by the central BH, or to resonant absorption in a diffuse plasma above the accretion disc (Ruszkowski & Fabian 2000).

We used the same dataset of Nandra *et al.* (1999)[d] and started constraining the continuum to the broad-band best-fit values: $n_H = 0.20 \times 10^{22}$ cm^{-2}, $\Gamma = 1.31$. Then we tried fitting with a simple powerlaw + kerrspec model. A good fit ($\chi^2_{\rm red} = 1.15$) is obtained using an intermediate primary source height ($h = 20m$) for a Schwarzschild-like assumption on the innermost radius ($r_1 \equiv 6m$), but the resulting outer radius is then quite low ($r_2 \simeq 10.9m$) which does indeed indicate that the emissivity is concentrated at the lowest disc radii, as found by Nandra *et al.* (1999). The iron line EW is $\sim$ 240 eV. When adding an absorption feature at 5.89 keV (Nandra *et al.* 1999) in the form of a Gaussian function with negative normalization, the χ^2 does not improve while the other fit parameters have negligible variations.

We also tried with different values of r_1: for $r_1 \equiv 1.23m$ (maximal Kerr assumption) we get $r_2 = 17.0m$ and $\chi^2_{\rm red} \simeq 1.16$; for the same r_1 and h "lowered" to $10m$ we have $r_2 = 9.7m$ and $\chi^2_{\rm red} \simeq 1.26$.

In the residuals we also noticed that a narrow feature remains around 6.4 keV; we thus tried inserting an additional Gaussian narrow line in the model (model = wabs(powerlaw + kerrspec + zgauss). Even if the χ^2 improves ($\chi^2_{\rm red} \simeq 1.07$), still the residual feature is not completely accounted for. From the results we cannot really discriminate between the two BH models (spinning or static). However, the interesting point here is in the values we got for the disc radii. In our very best fit results, as well as in all other computations we made, the best-fit radii are quite close to each other (e.g. $r_1 = 5.5m$ and $r_2 = 7.6m$), which does not seem very physical; but this may indicate that the emissivity law is really steep, as already found by Nandra *et al.* (1999), thus that the primary flux is very anisotropic – even if the fit does not improve when varying h – and concentrated in the innermost part of the accretion disc.

3.3 GRS 1915+105

GRS 1915+105 is a galactic superluminal jet source, well-known as an amazing object in the X-ray sky since its discovery by the WATCH experiment on GRANAT in 1992 (Castro-Tirado *et al.*, 1992). Is shows an extreme variability, ranging over all timescales (e.g. Belloni *et al.*, 1997, and references therein). This source has no optical counterpart because of the very large interstellar absorption, but weak variable radio/IR emission connected with the jets (Mirabel & Rodriguez 1994).

[d] http://tartarus.gsfc.nasa.gov/html/76028000/76028000.html

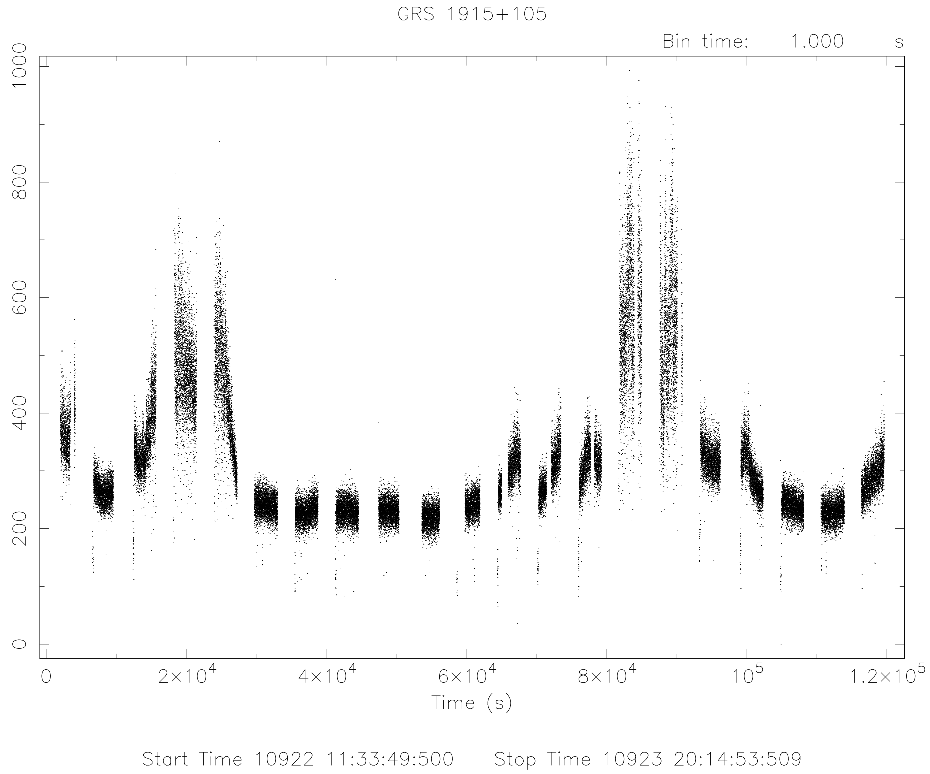

Figure 1. The lightcurve of GRS 1915+105 during the April 19, 1998 observation with *BeppoSAX*, which lasted $\sim$ 120 ks. The six spectral phases considered in this paragraph are those comprised between $t \sim 3 \times 10^4$ and $t \sim 6.2 \times 10^4$ s.

Table 3. Flux and duration of the six spectral phases sorted out from the *BeppoSAX* observation of GRS 1915+105 which took place on April 19th, 1998. The flux corresponds to the best-fit model in the energy interval from 3.5 to 8.0 keV.

	Flux:	[photons cm^{-2} s^{-1}]	[ergs cm^{-2} s^{-1}]	Count rate [cts/s]	Δt [s]
QS1	*maxim.*	2.084	1.627E-08	124	2562
QS2		1.963	1.541E-08	117	1993
QS3		2.026	1.592E-08	119	2551
QS4		1.990	1.575E-08	119	2003
QS5	*minim.*	1.889	1.489E-08	113	1628
QS6		2.072	1.617E-08	124	2708

Measurements of the jets superluminal motions allowed to estimate the source's distance $\sim$ 10 kpc and inclination $\sim$ 70 degrees. GRS 1915+105 is believed to host a BH because it shows properties very similar to those of the other famous "microquasar", GRO J1655-40, for which precise dynamical measurements yielded $M \sim 7M_\odot$, well above the standard neutron star mass limit.

GRS 1915+105 shows a strong iron Kα fluorescent emission line in the spectrum observed by *BeppoSAX* on April 19, 1998. Considering the time-averaged profile one obviously cannot get a meaningful fit because of the extreme source's variability. We therefore sorted out a phase of relative calmness in the lightcurve, and further divided this period into six short intervals (cp. table 3 and figure 1). We have

Table 4. Here is a summary of the best-fit results we obtained using the *BeppoSAX* observation of GRS 1915+105 which took place on 04/19/1998 (cp. table 3). While the continuum parameters T and Γ have been previously constrained to allow a faster computation with kerrspec, n_H^{bf}, h^{bf}, $r_{1,2}^{bf}$ are final best-fit values.

	n_H^{bf} [$\times 10^{22}$ cm^{-2}]	T [keV]	Γ	h^{bf}/m
QS1	5.89 ± 1.35	1.86 ± 0.46	2.91 ± 0.11	20.
QS2	6.34 ± 0.22	4.18 ± 0.08	3.13 ± 0.01	20.
QS3	5.39 ± 0.34	4.92 ± 0.27	2.68 ± 0.04	20.
QS4	5.68 ± 0.04	4.71 ± 0.07	2.71 ± 0.01	20.
QS5	5.85 ± 0.04	2.65 ± 0.21	3.32 ± 0.42	20.
QS6	6.02 ± 1.05	$1.94^{+0.48}_{-0.45}$	$2.94^{+0.30}_{-0.14}$	20.
	r_1^{bf}/m	r_2^{bf}/m	EW [eV]	$\chi^2_{\rm red}$
QS1	10.8 ± 2.3	49.4 ± 8.0	239.	1.55
QS2	11.5 ± 1.9	40.9 ± 5.4	282.	1.48
QS3	10.8 ± 4.3	36.4 ± 6.6	217.	1.40
QS4	1.230 frozen	372.7 ± 56.7	196.	0.91
QS5	12.5 ± 2.2	32.9 ± 5.0	269.	1.28
QS6	11.1 ± 1.6	35.4 ± 3.7	280.	0.89

fitted the data with a model wabs $\times$ diskbb(powerlaw + kerrspec). A summary of the results is shown in table 4.

In all six cases, the best fit is for an intermediate emissivity ($h = 20m$). When we exclude the spectrum QS4, which provided the biggest problems and uncertainties in the fitting (cp. table 4), in all the remaining cases we found no need for invoking a rotating BH. For all spectral phases the emitting disc region is the same within the errors – although interestingly the phases of minimum and maximum relative fluxes do also correspond to the minimally (QS5: $r_1 = 12.5$ and $r_2 = 32.9$) and maximally (QS2: $r_1 = 10.8$, $r_2 = 49.4$) extended best-fit emitting disc radii. However, more spectral phases should be analyzed in the future, in order to underline possible correlations which are not easily understandable at this stage, including also the reflection component in the model.

4 Conclusions

We showed preliminary results obtained with the kerrspec tool for some relevant sources: MCG–6-30-15, NGC 3516 and GRS 1915+105. We payed attention to the relativistic distortions on the iron line profiles, while fits performed including the continuum reflected component will be the subject of future work, to allow a complete coverage of the parameters space. These first computations have two main scopes: first, to test the feasibility of the newly developed numerical tool; secondly, to see whether the fast-spinning BH assumption is required by the data. In all cases, except for the MCG–6-30-15 deep minimum profile detected with *ASCA* (Iwasawa *et al.*, 1996) where light rays originating from below $6m$ are necessary to account for the extremely redshifted radiation, we found that a Schwarzschild model may explain the profile's time-averaged shape. In the case of the broad line profile detected in NGC 3516, on the base of our computations with kerrspec we can also confirm the previous claim (Nandra *et al.* 1999) that the emissivity law is very steep, which causes the best-fit disc emitting region to restrict to a narrow ring around $r_{eq} \sim 6m$.

The results are encouraging; however, the theoretical models still suffer from a large number of free parameters, which the observational evidence does not yet permit to constrain tightly enough. Better sensitivity and spectral resolution are needed to confirm the double-horn profiles expected in disc-type geometry under suitable conditions (e.g. large inclination angle), while temporal resolution will enable to perform reverberation mappings.

After the important results provided by the *ASCA* and *BeppoSAX* missions, many more data from the satellite *XMM-Newton*, launched in December 1999, will be available soon. These data have resolution comparable to that of *ASCA*, but a much better throughput. This will allow to get better insight of the known sources, and to increase the number of sources which may be profitably studied.

References

1. Belloni T. *et al.*, *Astroph. J.* **479**, L145 (1997).
2. Castro-Tirado A.J., Brandt S., Lund N., IAU Circular n.5590, 1992.
3. Done C., Nayakshin S., *Astroph. J.*, in press – astro-ph/0008292.
4. Fabian A.C. *et al.*, *MNRAS* **238**, 729 (1989).
5. Ghisellini G., Haardt F., Matt G., *MNRAS* **267**, 743 (1994).
6. Guainazzi M. *et al.*, *Astron. & Astroph.* **341**, L27 (1999).
7. Inoue H., *Exp. Astr.* **4**, 1 (1993).
8. Iwasawa K. *et al.*, *MNRAS* **282**, 1038 (1996).
9. Karas V., Vokrouhlický D., Polnarev A.G., *MNRAS* **259**, 569 (1992).
10. Laor A., *Astroph. J.* **376**, 90 (1991).
11. Martocchia A., Karas V., Matt G., *MNRAS* **312**, 817 (2000).
12. Martocchia A., Matt G., *MNRAS* **282**, L53 (1996).
13. Martocchia A., *X-Ray Spectral Signatures of Accreting Black Holes*, PhD Thesis, SISSA-ISAS, Trieste, October 2000.
14. Matt G., Perola G.C., Piro L., *Astron. & Astroph.* **247**, 25 (1991).
15. Mirabel I.F., Rodriguez L.F., *Nature* **371**, 46 (1994)
16. Molendi S. *et al.*, in: Proc. of the *X-Ray Astronomy 2000* Meeting, held in Mondello (PA), September 2000 – in preparation.
17. Nandra K. *et al.*, *Astroph. J.* **523**, L17 (1999).
18. Novikov I.D., Thorne K.S., in: *Black Holes*, ed. C. DeWitt & B. DeWitt, Gordon & Breach, New York, 1973.
19. Page D.N., Thorne K.S., *Astroph. J.* **191**, 449 (1974).
20. Ruszkowski M., Fabian A.C., *MNRAS* **315**, 223 (2000)
21. Tanaka Y. *et al.*, *Nature* **375**, 659 (1995).
22. Weaver K.A., Gelbord J., Yaqoob T., *Astroph. J.*, in press – astro-ph/0008522.